Chinese Journal of Catalysis 35 (2014) 1972–1981

available at www.sciencedirect.com

ScienceDirect

journal homepage: www.elsevier.com/locate/chnjc

Article

Role of aggregated Fe oxo species in N_2O decomposition over Fe/ZSM-5

Bo Zhang, Fudong Liu, Hong He *, Li Xue

Research Center for Eco-Environmental Sciences, Chinese Academy of Sciences, Beijing 100085, China

ARTICLE INFO

Article history:
Received 14 May 2014
Accepted 27 June 2014
Published 20 December 2014

Keywords:
N_2O decomposition
Fe/ZSM-5
Iron species
Thermal treatment

ABSTRACT

The effects of aggregated Fe oxo (FeO_x) species on N_2O decomposition activity of aqueous ion-exchanged Fe/ZSM-5 were investigated. Aggregation of FeO_x species was achieved by thermal treatment of the Fe/ZSM-5 catalysts at different temperatures (600–900 °C) in pure Ar. The characterizations were carried out using X-ray diffraction, N_2 physisorption, UV-Vis diffuse reflectance spectroscopy, X-ray absorption fine structure spectroscopy, pulse-response analysis, and O_2-temperature-programmed desorption. The FeO_x species on the external framework of the ZMS-5 zeolite played a dominant role in N_2O decomposition over Fe/ZSM-5. By studying the relationship between the contents of the various existing iron species and activity of the different catalysts, polynuclear FeO_x appeared to be the main active phase for N_2O decomposition. Additionally, Fe–O with a long bond length ($(Fe–O)_2$) in amorphous polynuclear FeO_x was positively correlated to the activity of the catalysts, indicating that $(Fe–O)_2$ was the active species for N_2O decomposition.

1. Introduction

Nitrous oxide (N_2O) is a greenhouse gas and major stratospheric source of NO_x contributing to ozone destruction [1,2]. Although N_2O is not a major contributor to global warming (~6%), its effect is much more potent than that of CO_2 and CH_4. Anthropogenic practices have led to a rapid increase in atmospheric N_2O concentrations, with an annual growth rate of 0.2%–0.3% [1]. Therefore, control of N_2O emissions from combustion and chemical processes has become a significant concern.

To control N_2O emissions from chemical processes, catalysts for N_2O decomposition have been widely studied in the last three decades. Among them, Fe/ZSM-5 [3–9] has been extensively studied owing to its remarkable activity and stability for N_2O decomposition even in the presence of relatively large amounts of O_2, NO, SO_2, and H_2O that are typical poisoning gases for other N_2O abatement catalysts. Fe/ZSM-5 has been traditionally prepared by aqueous ion exchange, solid-state ion exchange, and isomorphously substituted methods. Steaming [10–14] and thermal treatments [15–19] are beneficial for solid-state ion-exchanged and isomorphously substituted Fe/ZSM-5 for N_2O decomposition, and this has led to systematic investigations on the effect of steaming conditions on isomorphously substituted Fe/ZSM-5 [20–23]. Such research studies reported the key role of oligonuclear Fe oxo clusters or small intra-zeolitic Fe species on the external framework of the zeolite in N_2O decomposition, whereas Lewis and Brönsted acidic sites only play a minor role. Kaucký et al. [24] reported that both the short Fe–Fe distances and the presence of

* Corresponding author. Tel/Fax: 86-10-62849123; E-mail: honghe@rcees.ac.cn
This work was supported by the National High Technology Research and Development Program of China (863 Program, 2013AA065301), the National Basic Research Program of China (973 Program, 2010CB732304), and the National Natural Science Found for Creative Research Groups of China (51221892).
DOI: 10.1016/S1872-2067(14)60184-4 | http://www.sciencedirect.com/science/journal/18722067 | Chin. J. Catal., Vol. 35, No. 12, December 2014

Al-Lewis sites in the vicinity of Fe sites resulted in higher N_2O decomposition activity. Additionally, Dubkov[13] and Hensen et al. [18,19] determined that thermal treatment of solid-state ion-exchanged Fe/ZSM-5 in inert gas resulted in the reduction of some Fe^{3+} species to Fe^{2+} that promoted N_2O decomposition activity. However, rationalization of the advantages of such Fe/ZSM-5 treatments on N_2O-decomposition activity remains controversial.

Because of its convenient synthesis, aqueous ion-exchanged Fe/ZSM-5 has been considered one of the most promising candidates for the decomposition of N_2O emitted from industries. Certain types of iron species, such as iron ions and iron oxyhydroxide species, are prone to exchange with protons of zeolites. Moreover, $(FeO)_x$-Al on the external framework can form in channels following calcination of Fe/ZSM-5 [25–27]. Previous research studies reported on the performance optimization of aqueous ion-exchanged Fe/ZSM-5 using varying solutions and iron sources [25,27]. The effect of thermal treatment on solid-state ion-exchanged and isomorphously substituted Fe-ZSM-5 has been studied by Pérez-Ramírez and Hensen et al. However, the influence of thermal treatment on aqueous ion-exchanged Fe/ZSM-5 relating to N_2O decomposition activity is not well understood.

Herein, Fe/ZSM-5 catalysts were thermally treated in the temperature range of 600 to 900 °C in Ar. The effects of thermal treatment on the structure of Fe oxo species and textural properties of Fe/ZSM-5 were considered and characterizations were performed accordingly. To achieve varying types of iron species during thermal treatment, Fe/ZSM-5 with 2.6 wt% Fe (Fe/Al molar ratio = 1) was prepared by the aqueous ion-exchange method.

2. Experimental

2.1. Catalyst preparation

Fe/ZSM-5 catalysts were prepared by ion-exchange from aqueous solution. Briefly, HZSM-5 zeolite, with Si/Al molar ratio = 36, was added to Fe(III) nitrate aqueous solution at 90 °C. After vigorous stirring, the sample was washed and dried in air at 100 °C for one night (referred to as non-calcined Fe/ZSM-5). The non-calcined Fe/ZSM-5 was then calcined at 550 °C in air for 3 h (referred to as Original). Fe/ZSM-5 prepared with 2.6 wt% Fe (Fe/Al molar ratio = 1) was treated in the temperature range of 600–900 °C in pure Ar. The resulting thermally treated catalysts are referred to as FZT (where T refers to the temperature employed). X-ray diffractometry measurements of the samples, as described below, showed that the MFI zeolite structure was retained after the high-temperature treatments.

2.2. Catalyst characterization

The chemical composition (including the concentration of Fe) of the catalysts was determined by atomic absorption spectrometry (AAS; Shimadzu, AA6300).

Catalysts were characterized by X-ray diffraction (XRD) using a computerized Rigaku D/max-RB diffractometer (Japan, Cu K_α radiation, 0.154056 nm). Scans were taken from 2θ = 10° to 2θ = 90° at a speed of 4°/min. The accelerating voltage and the applied current were 40 kV and 300 mA, respectively.

The nitrogen adsorption-desorption isotherms were obtained at −196 °C on a Quantasorb-18 automatic instrument (Quanta Chrome Instrument Co.). Prior to measurements, samples were evacuated at 300 °C for 10 h. Specific areas were computed from the sorption isotherms using the Brunauer-Emmett-Teller (BET) method.

UV-Vis diffuse reflectance spectroscopy (DRS) was conducted on a U-3010 spectrophotometer (Hitachi) equipped with a standard diffuse reflectance unit under ambient conditions. The scanning range was 190–800 nm and the scan rate was 300 nm/min. HZSM-5 was used as a reference material. The measured spectra were converted into Kubelka-Munk functions and deconvoluted into Gaussian sub-bands that could be quantitatively assigned to the different iron species present in the prepared samples.

Fe K-edge X-ray absorption fine structure (XAFS) of the samples was measured on a BL14W1 beamline at the Shanghai Synchrotron Radiation Facility (China). The storage ring was operated at 3.5 GeV with a ring current of 200 mA. A single Si (111) crystal was used to generate a monochromated X-ray beam. The spectra were recorded with sampling steps of 0.5 eV in the X-ray absorption near edge structure (XANES) region and 1–5 eV in the extended X-ray absorption fine structure (EXAFS) region. The Fe K-edge spectra were recorded in fluorescence mode under ambient conditions and the effect of fluorescence saturation was assessed using α-Fe_2O_3 as a reference. The EXAFS data were extracted from the measured absorption spectra with the XDAP code. The pre-edge was subtracted using a modified Victoreen curve, and the background was subtracted using cubic spline routines. Finally, normalization was performed by dividing the subtracted absorption spectra by the intensity of the absorption spectrum at 50 eV above the Fe K-edge. Structural information was determined by multi-shell fitting in R space [28]. The fits were assessed by k^1 and k^3 weighting. Errors were estimated at ±10% for the coordination numbers (N), ±1% for the coordination distances (R), ± 5% for the Debye–Waller factor (σ^2), and ±10% for the inner-potential correction (E_0).

2.3. Steady-state studies

Activity measurements were carried out in a fixed-bed quartz flow reactor (internal diameter, 4 mm), containing ~50 mg catalyst (particle size, 125–200 μm) in all experiments. The reactor was heated by a temperature-controlled furnace. A thermocouple was placed on the external surface of the reactor tube. A N_2O (0.15 vol%) reaction mixture was introduced into the reactor at a gas hourly space velocity (GHSV) of 35 000 h^{-1}. Analysis of the reaction products was carried out by gas chromatography (Agilent 6890N equipped with Porapak Q for the analysis of N_2O and CO_2, and molecular sieve 5A columns for the analysis of N_2, O_2, and NO). The reaction system was maintained at the selected reaction temperature for 1 h to reach

steady state prior to product analysis. In all tests, N_2 and O_2 were the only gaseous products observed.

The apparent activation energy (E_a) and the turnover frequency (TOF) were calculated [26] from the following equations:

$$E_a = d(\ln k)/d(1/T) \quad (1)$$

$$TOF = kp_{N2O}/n_{Fe} \quad (2)$$

where k is the first-order rate constant and n_{Fe} is the number of active iron obtained from the O_2-temperature-programmed desorption (O_2-TPD) studies, as described in section 2.4.

2.4. O_2-TPD studies

The O_2-TPD experiments were performed under a He (50 cm³/min) flow over 300 mg catalyst and a heating rate of 30 °C/min. Prior to the experiment, the catalysts were pretreated under a flow of 2% N_2O/Ar for 1 h, followed by cooling to 150 °C under the same flow. The adsorbed oxygen species remained on the surface after N_2O decomposition over the catalyst, and were detected using a mass spectrometer (Hiden).

2.5. Pulse-response studies

For the N_2O pulse-response experiments, a six-port switching valve was installed in front of the reactor to periodically change between 2 vol% N_2O/He and pure He atmospheres. Prior to the experiment, the decomposition of N_2O over the catalyst was maintained at 500 °C for 1 h to reach steady state. The periodical switching between 2% N_2O/He and pure He was performed at intervals of 4 min. A similar procedure was adopted in the air pulse-response experiments to compare the diffusion rate of N_2 with that of O_2 in the catalyst bed.

3. Results and discussion

3.1. Steady-state N_2O decomposition

Figure 1 shows the steady-state conversions of N_2O as a function of temperature over the original and thermally treated Fe/ZSM-5 catalysts. As observed, thermal treatment significantly improved the activity of Fe/ZSM-5 catalysts. Among the prepared catalysts, FZ750, treated at 750 °C, achieved 100% N_2O conversion at the lowest reaction temperature studied. Thus, 750 °C was regarded as the optimal treatment temperature. FZ850 featured considerably higher activity than FZ800 and FZ750 in the low-temperature reaction region, whereas FZ750 exhibited the best activity for N_2O decomposition in the high-temperature reaction region. This suggests the occurrence of complex transformations in the active species structure during the thermal treatment process.

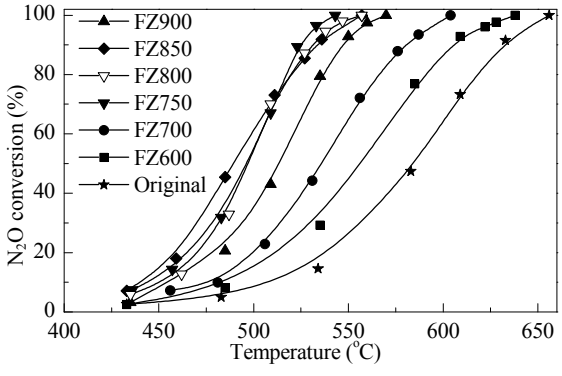

Fig. 1. Activity of the original and thermally treated Fe/ZSM-5 catalysts towards N_2O decomposition. Feed composition: 0.15 vol% N_2O; balance He; GHSV = 35000 h⁻¹.

3.2. N_2 adsorption-desorption studies

N_2 adsorption was performed to investigate the textural properties of HZSM-5 and Fe/ZSM-5 catalysts. The N_2 adsorption-desorption isotherms exhibited high N_2 uptakes at low relative pressures and a plateau at high relative pressures (Fig. 2). The isotherms were classified as Type I according to IUPAC classification for microporous materials [29] that is typical of HZSM-5, as investigated in a previous research study [20]. The surface area and total pore volume of the original and thermally treated Fe/ZSM-5 catalysts were calculated from the corresponding N_2 adsorption-desorption isotherms, and are listed in Table 1. Upon Fe species exchange with protons, N_2 uptake of the non-calcined Fe/ZSM-5 sample decreased (Fig. 2). Accordingly, the surface area and total pore volume of non-calcined Fe/ZSM-5 decreased (Table 1). It was likely that some Fe oxide species incorporated into the zeolite channel during the ion-exchange process, thus reducing N_2 uptake on non-calcined

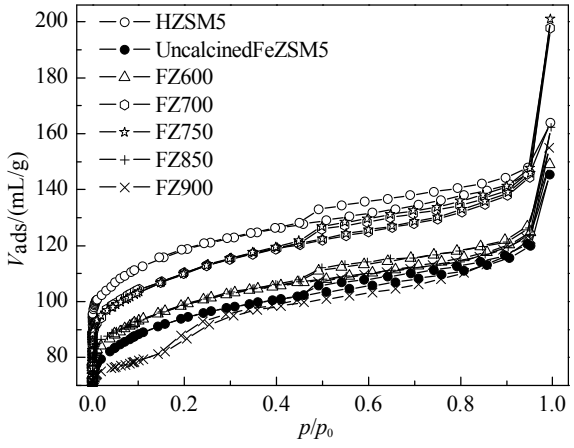

Fig. 2. N_2 adsorption-desorption isotherms of HZSM-5, and non-calcined and thermally treated Fe/ZSM-5 catalysts.

Table 1
Textural properties of HZSM-5, and non-calcined and thermally treated Fe/ZSM-5 catalysts.

Sample	S_{BET}/(m²/g)	V_{total}/(cm³/g)
HZSM-5	371	0.254
Non-calcined Fe/ZSM-5	287	0.225
FZ600	302	0.231
FZ700	342	0.307
FZ750	343	0.312
FZ800	325	0.310
FZ850	306	0.252
FZ900	279	0.237

Fe/ZSM-5 [19]. Treatment temperatures below 750 °C instigated partial migration of small Fe species from the micropore to the external surface of the zeolite, thereby increasing the catalyst pore volume. In contrast, treatment temperatures above 750 °C resulted in the aggregation of FeO_x clusters and collapse of the ZSM-5 zeolite framework, subsequently blocking the channels in FZ800, FZ850, and FZ900 that was responsible for the low total pore volume and surface area [19].

3.3. XRD analysis

The XRD patterns of HZSM-5 and thermally treated Fe/ZSM-5 catalysts are shown in Fig. 3. All catalysts displayed highly crystalline ZSM-5 features, as indicated by the strong intensity of the characteristic peaks and the weak background noise in the XRD patterns. These results suggest that the different treatment temperatures employed did not degrade the crystalline structure of the ZSM-5 zeolite.

Hensen et al. [19] reported that severe calcination conditions could induce growth and ordering of the Fe oxide aggregates in Fe/ZSM-5, as prepared by chemical vapor deposition of $FeCl_3$. As observed in Fig. 3, distinct hematite peaks were not observed in FZ600 and FZ700, indicating that the Fe oxides on the catalysts were mainly amorphous. Crystalline Fe_2O_3 was observed in catalysts FZ750, FZ800, FZ850, and FZ900. To further assess the distribution of the FeO_x species, the following experiments were conducted.

3.4. UV-Vis DRS studies

The nature and distribution of the Fe species on the catalysts were investigated by UV-Vis DRS spectroscopy. The obtained spectra were converted into Kubelka-Munk functions and assigned to Fe^{3+}←O charge-transfer bands, as shown in Fig. 4. Bands between 190 and 305 nm were attributed to isolated Fe^{3+} species (Fe_1), which are tetrahedrally coordinated within the zeolite framework (band below 250 nm) and with higher coordination (band within 244–305 nm). Octahedral Fe in small oligonuclear Fe oxide species generated bands between 305 and 400 nm (Fe_2). Bands above 400 nm were attributed to

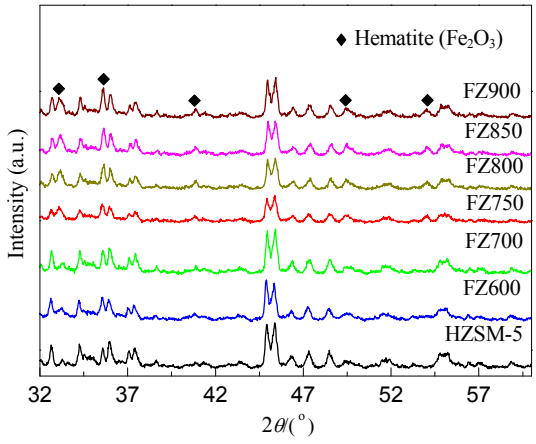

Fig. 3. XRD patterns of HZSM-5 and thermally treated Fe/ZSM-5 catalysts.

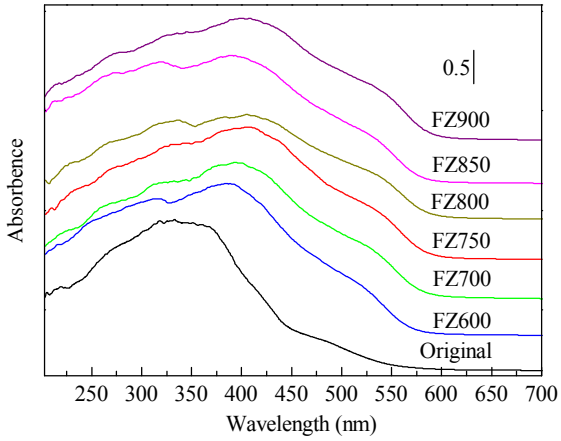

Fig. 4. UV-Vis DRS spectra of the original and thermally treated Fe/ZSM-5 catalysts.

characteristic asymmetric peaks of large Fe oxide particles. Bands between 400 and 500 nm were attributed to polynuclear Fe oxide (Fe_3) and bands above 500 nm were characteristic of large Fe oxide particles without N_2O decomposition activity [19,23,30]. Based on the work of Pérez-Ramirez et al. [23,30], a semiquantitative estimation of the distribution of the Fe species in the zeolite was performed by deconvoluting spectra into Gaussian sub-bands, as shown in Table 2 and Fig. 5.

Most of the Fe species in non-calcined Fe/ZSM-5 were octahedral Fe^{3+} and oligonuclear Fe oxide [30], most probably derived from the ion-exchange process (Fig. 4). In contrast, bulk Fe oxide species were observed in the high-temperature-treated catalysts, as evidenced by the band at ~400 nm. It is interesting to note that the intensity of bands between 400 and 500 nm (I_3) initially increased and then decreased with increasing treatment temperatures (Table 2). As previously mentioned, Fe oxide aggregates on the external surface during high-temperature treatments [19,24,27]. Based on the XRD results, the presence of the inflexion points was due to several reasons: thermal treatment below 750 °C promoted the aggregation of amorphous Fe oxide; the transformation of FeO_x species from the amorphous to the crystalline state within the 750–850 °C treatment resulted in a reduced volume of FeO_x particles; and the aggregation of crystalline Fe oxide particles increased I_3 observed for FZ900. The current findings suggested that thermal treatment likely instigated aggregation in both

Table 2
Area ratios of the sub-bands (I_1 at λ < 300 nm, I_2 at 300 < λ < 400 nm, and I_3 at 400 < λ < 500 nm) estimated by deconvolution of UV-Vis DRS spectra of the original and thermally treated Fe/ZSM-5 catalysts.

Sample	I_1 [a] (%)	I_2 [b] (%)	I_3 [c] (%)
Non-calcined Fe/ZSM-5	22	65	13
FZ600	22	36	42
FZ700	8	47	45
FZ750	18	31	51
FZ800	18	33	49
FZ850	14	39	47
FZ900	12	39	49

[a] Isolated Fe^{3+} in tetrahedral and higher coordination. [b] Oligonuclear Fe oxide species. [c] Polynuclear Fe oxide species.

the amorphous and crystalline Fe oxides. The trend observed for I_3 that was in accordance with catalyst activity suggested that the polynuclear Fe oxide species, among all Fe oxide species identified, were the most active towards N_2O decomposition.

3.5. XAFS studies

The original and thermally treated Fe/ZSM-5 catalysts, and Fe_2O_3, FeO, and Fe foil reference compounds were thoroughly examined by XAFS, including XANES and EXAFS. XANES is a fingerprint technique that allows identification of the oxidation state and coordination environment provided availability of a suitable model compound [25,31]. The normalized Fe K-edge XANES profiles are shown in Fig. 6(a). The absence of a pre-edge absorption was due to the forbidden 1*s*→3*d* transition in octahedral coordinations [19]. The weak peak at ~7140 eV, corresponding to 1*s*→4p_z transition, suggests that only the distorted octahedral symmetry of the oxide of Fe^{3+} was present in the samples [19]. Fig. 6(b) shows the first derivative of the Fe K-edge XANES profiles of the original and thermally treated Fe/ZSM-5 catalysts, and Fe_2O_3, FeO, and Fe foil. The similarity

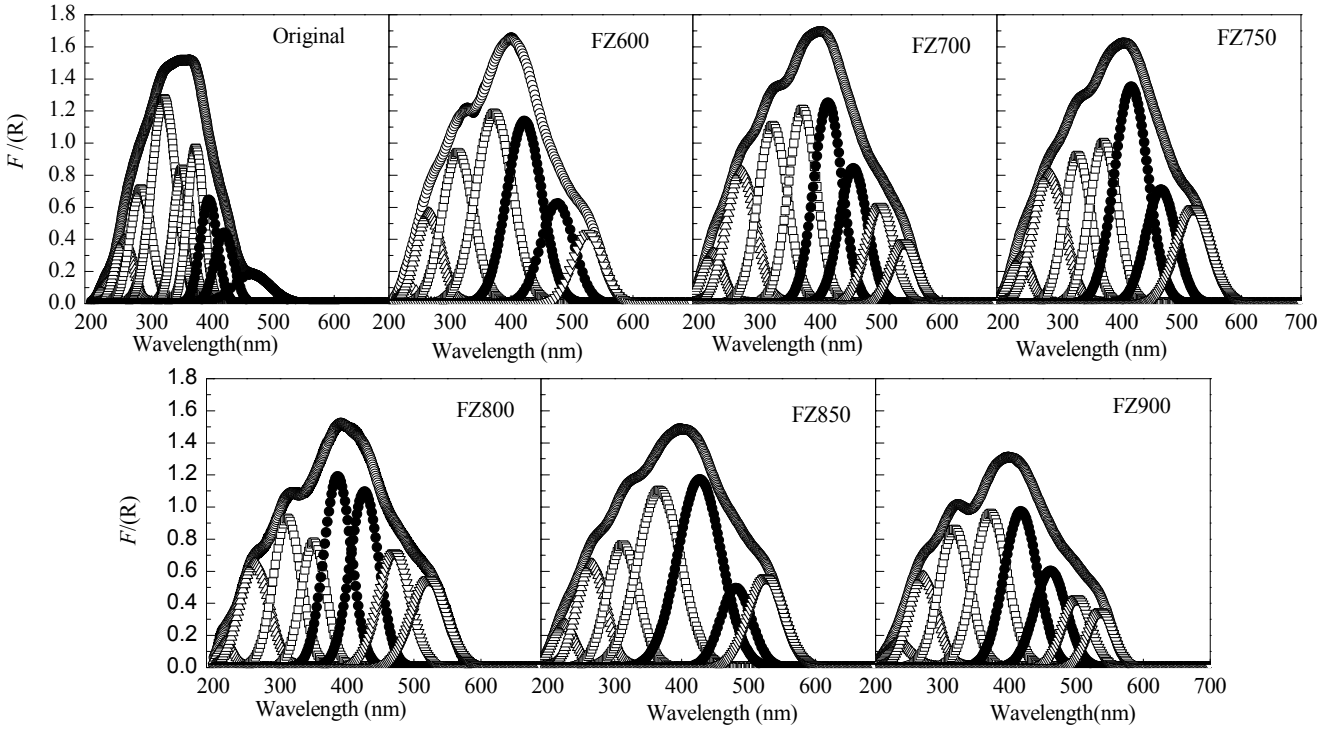

Fig. 5. UV-Vis DRS spectra and deconvoluted sub-bands of the original and thermally treated Fe/ZSM-5 catalysts. (△) isolated Fe^{3+} in tetrahedral and higher coordination, $\lambda < 300$ nm; (□) oligonuclear Fe oxide species, $300 < \lambda < 400$ nm; (•) polynuclear Fe oxide species, $400 < \lambda < 500$ nm; (▽) bulk Fe oxide species, $\lambda > 500$ nm.

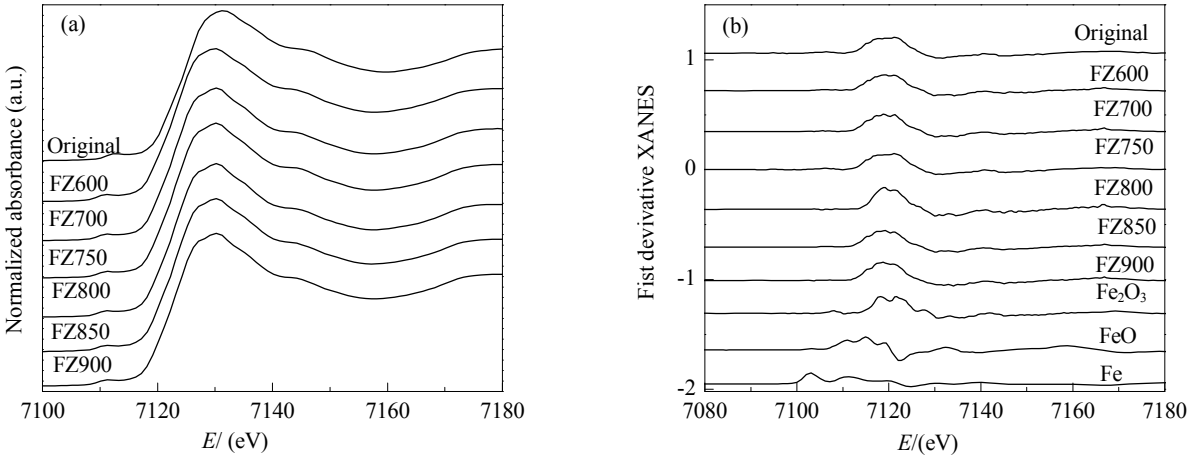

Fig. 6. (a) Normalized Fe K-edge XANES spectra of the original and thermally treated Fe/ZSM-5 catalysts. (b) First-derivative profiles of the Fe K-edge XANES spectra of the original and thermally treated Fe/ZSM-5 catalysts, and Fe_2O_3, FeO, and Fe foil.

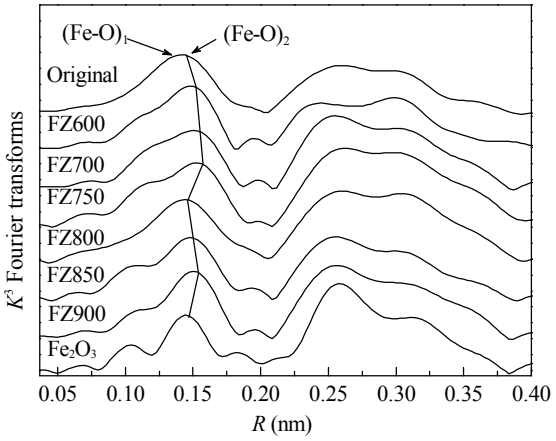

Fig. 7. Fourier transforms of the k^3-weighted Fe K-edge EXAFS oscillations for the original and thermally treated Fe/ZSM-5 catalysts.

between the spectra of the Fe/ZSM-5 catalysts and Fe_2O_3 indicates that the Fe species in the Fe/ZSM-5 catalysts are not reduced during thermal treatment in Ar.

Fe K-edge EXAFS analysis provides information on the structural environment of the Fe species in the original and thermally treated Fe/ZSM-5 catalysts [31]. Fig. 7 shows the k^3-weighted Fourier transforms of EXAFS oscillations into R space. The spectra of the original and thermally treated Fe/ZSM-5 catalysts were obviously and significantly different from each other, including their peak position and intensity. In R space, an asymmetric peak was apparent at ~0.16 nm, which was attributed to the six oxygen atoms in the first Fe–O coordination shell [31]. The contribution at 0.25 nm was ascribed to considerable scatter and fitted with the Fe–Fe shell. Multi-shell analysis of the EXAFS data was performed using the models proposed by Battiston et al. [31]. The Fe–O and Fe–Fe references were calibrated for the EXAFS data obtained from hematite Fe_2O_3 by fitting in R space (see Table 3). In particular, the first oxygen-coordination shell was fitted at two different distances, 0.191 nm $(Fe–O)_1$ and 0.20 nm $(Fe–O)_2$. However, during the curve fitting process, the number of oxygen atoms in the first coordination shell was not always fitted to six, suggesting the existence of Fe–OH [31]. The second coordination shell can be fitted with two Fe–Fe. The fitting results are listed in Table 4. For ease of comparison between the experimental data and curve fitting results, the Fourier transforms of k^3-weighted EXAFS oscillations and the corresponding fitting curves are presented in Fig. 8.

Table 3
Crystallographic data used to produce the EXAFS reference files.

Atom pair	Coordination number (CN)	R (nm)
$(Fe–O)_1$	3.0	0.195
$(Fe–O)_2$	3.0	0.212
$(Fe–Fe)_1$	3.0	0.297
$(Fe–Fe)_2$	3.0	0.336

Table 4
Fitting parameters of the multi-shell analysis of the Fe K-edge EXAFS of the original and thermally treated Fe/ZSM-5 catalysts.

Sample	$(Fe–O)_1$		$(Fe–O)_2$		$(Fe–Fe)_1$		$(Fe–Fe)_2$	
	CN	R (nm)	CN	R (nm)	CN	R (nm)	CN	R (nm)
Original	3.0	0.191	3.0	0.21	0.9	0.279	2.7	0.300
FZ600	3.2	0.191	2.2	0.21	2.9	0.30	3.6	0.335
FZ700	2.1	0.194	2.6	0.20	3.2	0.295	3.0	0.330
FZ750	1.8	0.191	3.6	0.21	4.0	0.293	3.0	0.338
FZ800	2.2	0.191	3.0	0.21	5.0	0.293	3.0	0.338
FZ850	2.2	0.191	3.0	0.21	6.0	0.294	3.0	0.338
FZ900	3.6	0.196	2.6	0.20	7.3	0.299	3.0	0.338

Coordination numbers (CN) are accurate to ±10% and interatomic distances (R) are accurate to ±0.002 nm. Debye-Waller factors are typically in the range of 0.00005–0.00025 nm^2.

Table 4 shows that thermal treatment greatly influenced the coordination number and slightly changed the bond lengths of Fe–O and Fe–Fe. Thermal treatment induced agglomeration and ordering of iron oxide, as reflected by the increasing Fe–Fe coordination numbers. The $(Fe–O)_2$ bond coordination number showed a similar changing trend to that related to the catalysis

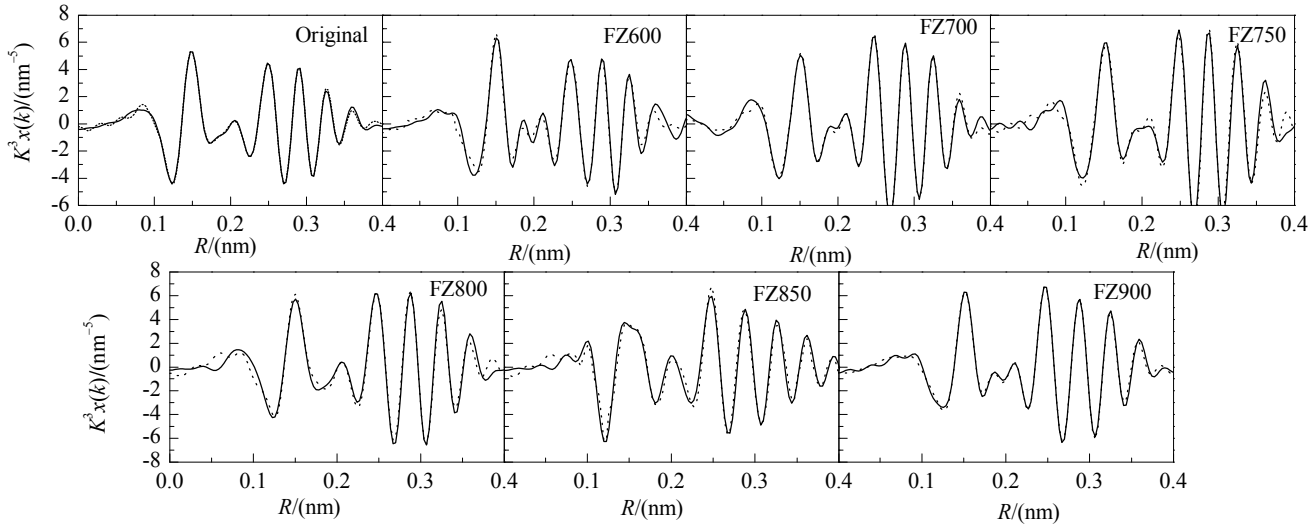

Fig. 8. Fourier transforms of k^3-weighted EXAFS oscillations (solid line) and the corresponding fitting curves (dotted line) for the original and thermally treated Fe/ZSM-5 catalysts.

activity with increasing thermal treatment temperatures, indicating that $(Fe–O)_2$ was the active species for this reaction.

3.6. Pulse-response experiment

The catalytic N_2O decomposition reaction involves the adsorption of N_2O at the active catalytic site followed by decomposition, resulting in the formation of N_2 and surface oxygen. The surface oxygen can be desorbed upon reaction with another oxygen atom or another N_2O. The four steps are shown in the following Eqs.:

$$N_2O + * \leftrightarrow N_2O* \quad (3)$$

$$N_2O + * \rightarrow N_2 + O* \quad (4)$$

$$N_2O + O* \rightarrow N_2 + O_2 + 2* \quad (5)$$

$$O* + O* \rightarrow O_2 + 2* \quad (6)$$

The rate of O_2 desorption is known to influence the activity of the catalyst [18]. The rate-limiting step is either that shown in Eq. (5) or in Eq. (6) depending on the catalyst.

In this study, the characterization and activity tests demonstrated that the long bond length $(Fe–O)_2$ in the Fe oxide particles was likely advantageous to the activity of the catalysts. To examine the relationship between the intrinsic mechanism of N_2O decomposition and the role of $(Fe–O)_2$ in Fe oxides, pulse-response and O_2-TPD experiments were conducted.

N_2O decomposition is initiated upon activation of N_2O on the active site, leading to adsorbed O species (α-O), Eq. (4). Two different mechanisms are postulated for the regeneration of the active site: reaction between another N_2O molecule and the oxidized site, Eq. (5), and the recombination of adsorbed oxygen atoms, Eq. (6). To discriminate between these two alternative reactions pathways, pulse-response experiments were performed by pulsing either N_2O or air.

Fig. 9(a) shows the response of the N_2O pulse over catalyst FZ750. Other samples showed similar behaviors to FZ750. As clearly observed, the evolution of molecular oxygen was delayed when compared with that of N_2. As shown in Fig. 9(b), N_2 and O_2 evolved at the same time in the air pulse study, indicating the absence of different diffusion rates of N_2 and O_2 in the bed of catalysts. These results demonstrate that the generated rate of diffusion of O_2 is lower than that of N_2 in N_2O decomposition. According to Sun et al. [15], the recombination of adsorbed oxygen atoms, Eq. (6), is the limiting step of the catalytic N_2O decomposition process.

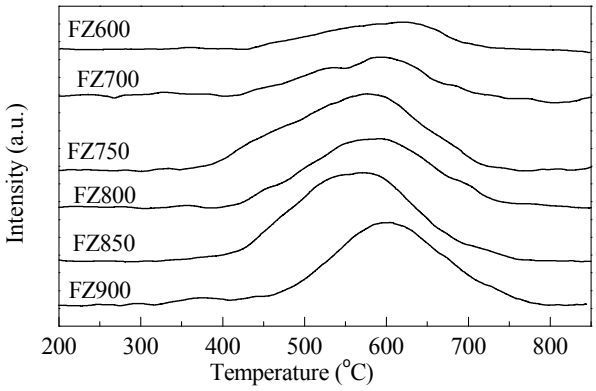

Fig. 10. O_2-TPD profiles of the thermally treated Fe/ZSM-5 catalysts after exposure to 2% N_2O at 485 °C.

3.7. O_2-TPD experiment

Fig. 10 shows the O_2-TPD profiles of the thermally treated Fe/ZSM-5 catalysts pretreated with 2% N_2O at 485 °C for 1 h. The broad peak obtained at 400–800 °C was ascribed to the desorption of α-O, which was formed upon decomposition of N_2O. As observed in Fig. 10, the trend of the O_2 desorption temperature was consistent with that of the activity of the catalysts, confirming the importance of O_2 desorption to the activity of the catalysts. For better comparison, the number of effective Fe sites (C_{Fe}) calculated according to the amount of the desorbed O_2 and turnover frequency (TOF) of N_2O decomposition over each active site are listed in Table 5. FZ750 displayed the highest concentration of active iron (C_{Fe}), whereas FZ900 featured the highest TOF among all Fe/ZSM-5 catalysts. The trend of C_{Fe} was proportionally correlated to the activity of the catalysts, indicating that the number of active sites (n_{Fe}) determined the activity of catalysts. The high activity of FZ750 was likely because of the high amount of $(Fe–O)_2$. The crystalline Fe oxide likely promoted N_2O decomposition. In contrast, smaller values of C_{Fe} reduced the apparent activity of the catalysts.

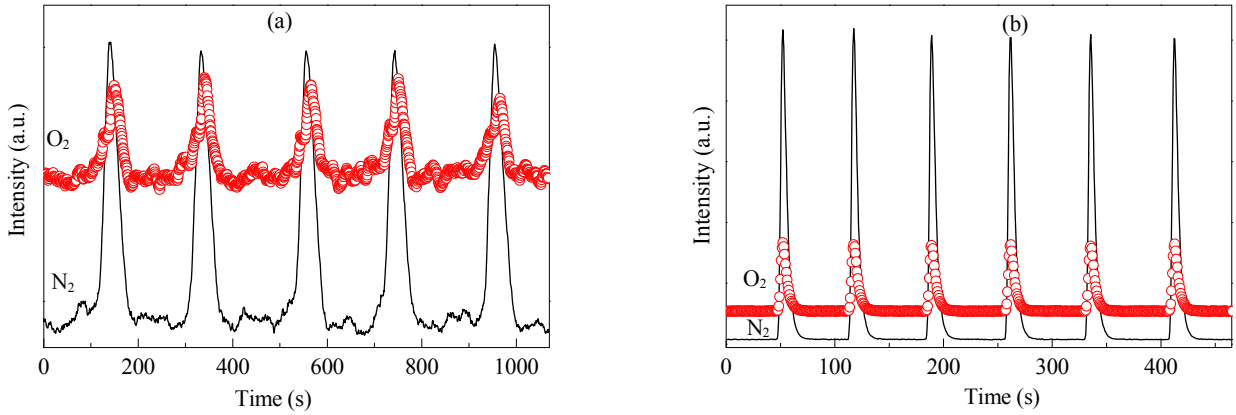

Fig. 9. Pulse-response profiles obtained by periodically switching (a) 2 vol% N_2O or (b) air to He over FZ750 catalyst at 485 °C.

Table 5
Concentration of active sites (C_{Fe}) in the thermally treated Fe/ZSM-5 catalysts and associated calculated turnover frequencies (TOF) during N_2O decomposition at 485 °C.

Sample	C_{Fe} [a] (μmol/g)	TOF (ks^{-1})
Original	10.2	7.2
FZ600	12.9	6.9
FZ700	17.1	6.3
FZ750	41.5	7.2
FZ800	39.0	7.7
FZ850	38.4	8.3
FZ900	38.0	9.7

[a] Obtained from the O_2-TPD experiment.

3.8. Discussion

3.8.1. Effect of high-temperature treatment in Ar on FeO_x in Fe/ZSM-5

The nature of Fe oxide strongly influenced the catalytic activity of Fe/ZSM-5 towards N_2O decomposition. Based on the XRD data, two different typologies of FeO_x present in the catalysts were considered: (1) amorphous state and (2) crystalline state. The UV-Vis DRS results showed that aggregation of the two FeO_x species increased with increasing treatment temperatures. The FeO_x aggregation phenomenon was in accordance with earlier observations of Fe/ZSM-5 treated under high temperatures [19,25,27].

In this study, aggregation of amorphous and crystalline FeO_x showed different influence on the activity of the thermally treated Fe/ZSM-5 for direct N_2O decomposition. At treatment temperatures below 750 °C, FeO_x was amorphous. The activity of the catalysts improved with increasing treated temperatures, indicating that aggregation of amorphous FeO_x improved the activity of the catalysts. Based on the UV-Vis DRS spectra, XAFS, and O_2-TPD results of the thermally treated Fe/ZSM-5 catalyst, the long $(Fe–O)_2$ bond length in the amorphous polynuclear FeO_x species promoted the activity of catalysts, indicating that $(Fe–O)_2$ was the active species. At treatment temperatures above 750 °C, crystalline FeO_x in the Fe/ZSM-5 catalysts aggregated with increasing treated temperatures. Although the intrinsic activity of crystalline FeO_x was higher than that of the amorphous FeO_x, as observed from the TOF data, increasing amounts of active Fe–O bonds were sealed in the bulk of crystalline FeO_x with increasing treated temperatures, thereby leading to reduced C_{Fe} values and decreased catalyst activity.

3.8.2. Thermodynamic origin of the enhanced activity of the Fe/ZSM-5 catalysts towards N_2O decomposition

The rate of N_2O decomposition and correlations of thermodynamic parameters are given as follows [18,26,32]:

$$r = kp^n_{N2O} = A\exp(-E_a/RT)p^n_{N2O} \quad (7)$$

$$A = k_B T/h \exp(\Delta_r^{\ddagger}S_m^{\theta}) \quad (8)$$

where r is the rate of N_2O consumption, k is the rate coefficient, k_B is the Boltzmann constant (1.38×10^{-23} J/K), h is the Plank constant (6.626×10^{-34} J·s), T (K) is temperature, A is the pre-exponential factor, E_a is the apparent activation energy, n is the order of reaction, and $\Delta_r^{\ddagger}S_m^{\theta}$ is the standard molar entropy of activation. The linear relationship between the reaction rate

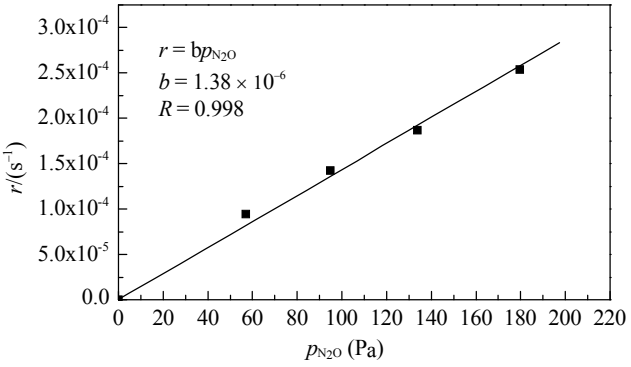

Fig. 11. Relationship between the reaction rate (r) and partial pressure of N_2O (p_{N2O}) of FZ750 catalyst. Reaction conditions: total flow rate, 50 cm^3/min; W/F, 0.06 g·s/cm^3; temperature, 400 °C; gas composition, 0.05 vol%–0.2 vol% N_2O; N_2O conversion percentage < 10%.

(r) and N_2O partial pressure (p_{N2O}) in Fig. 11 indicates that the decomposition of N_2O over FZ750 catalyst is a first-order reaction. Findings from previous research studies [18,26] also indicated that N_2O decomposition is a first-order reaction (n = 1). Arrhenius plots obtained from the steady-state N_2O decomposition (below 20% conversion efficiency) over the thermally treated Fe/ZSM-5 catalysts are shown in Fig. 12. Kinetic parameters for the catalysts were calculated from Arrhenius plots under the assumption of first-order disappearance of nitrous oxide, as shown in Table 6. The accuracy of E_a was ±10 kJ/mol.

From Table 6, the apparent activation energy E_a and apparent pre-exponential factor A of the catalysts were substantially different. As seen, E_a increased from 139 kJ/mol for FZ600 to 209 kJ/mol for FZ750, and then decreased to 105 kJ/mol for FZ900. Simultaneously, A increased from 3.0×10^5 to 7.9×10^{10}, and then declined to 5.3×10^3 s^{-1}·Pa^{-1}. The values of E_a were proportional to ln$A$ values of the catalysts (Fig. 13) that can be well explained by the compensation effect [33]. Based on the steady-state activity of the catalysts towards N_2O decomposition, A was a better determining factor than E_a to the activity of the catalysts. Equation (6) shows that $\Delta_r^{\ddagger}S_m^{\theta}$ of the various transition state species (e.g., α-O) plays an important role in determining the value of A. Based on these analyses, the standard molar entropy $\Delta_r^{\ddagger}S_m^{\theta}$ of α-O and the active sites were the major factors influencing the reaction rate.

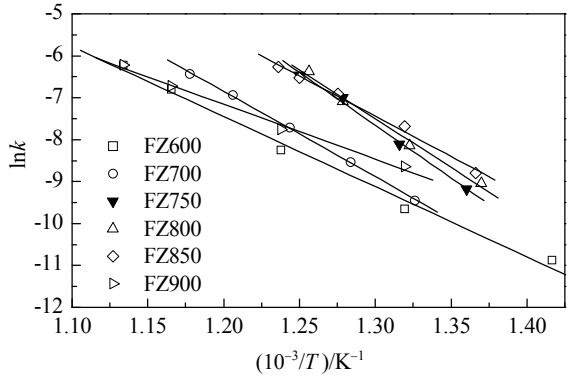

Fig. 12. Arrhenius plots of N_2O decomposition over the thermally treated Fe/ZSM-5 catalysts.

Table 6
Apparent activation energy (E_a) and pre-exponential factor (A) for N_2O decomposition over the thermally treated Fe/ZSM-5 catalysts.

Sample	E_a (kJ/mol)	A (s^{-1} Pa^{-1})
Original	105	7.0×10^3
FZ600	139	3.0×10^5
FZ700	169	4.4×10^7
FZ750	209	7.9×10^{10}
FZ800	194	7.7×10^9
FZ850	159	3.9×10^7
FZ900	105	5.3×10^3

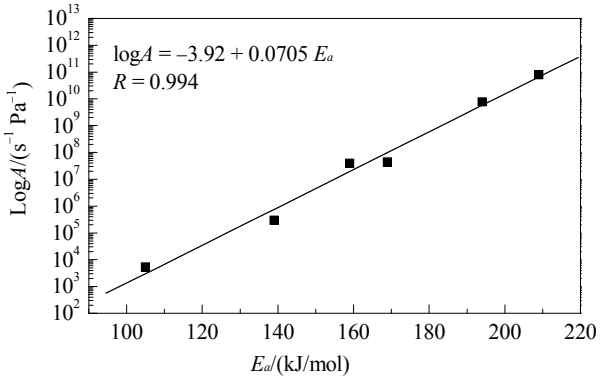

Fig. 13. Plot of ln$A$ as a function of E_a for N_2O decomposition over the thermally treated Fe/ZSM-5 catalysts.

The structure of the active site likely influenced the value of active entropy of the transition state of α-O. When α-O deviates from the Fe active sites, prior to rupture of the bond $(Fe–O)_2$, the latter donates electron to α-O because the bond energy of $(Fe–O)_2$ species is lower than that of $(Fe–O)_1$ species, thereby confirming the hypothesis that $(Fe–O)_2$ species are the active species.

Based on the value of A, $(Fe–O)_2$ species promoted the activity of the catalysts by increasing the entropy of the transition state of α-O. The higher the amount of active sites on the catalyst, the larger the total value of active entropy. Therefore, FZ750 that possessed the highest amount of $(Fe–O)_2$ had the highest activity towards N_2O decomposition.

The polynuclear Fe oxide species facilitate the recombination of adsorbed oxygen atoms in contrast to the oligonuclear Fe oxide species. $(Fe–O)_2$ existed in both the oligonuclear and polynuclear Fe oxide species. However, the higher amount of $(Fe–O)_2$ species in the polynuclear Fe oxide species was beneficial to enhancing the activity of the catalysts. For example, CN of $(Fe–O)_2$ and the content of the oligonuclear Fe oxide species in the original Fe/ZSM-5 catalyst were both high. However, C_{Fe} was low. Therefore, the number of $(Fe–O)_2$ in the polynuclear FeO_x species determined the C_{Fe} of the catalysts, which was estimated by multiplying CN of $(Fe–O)_2$ by the content of the amorphous polynuclear FeO_x species.

4. Conclusions

The aggregation of FeOx species on the external framework of ZSM-5 zeolite during thermal treatment played a dominant role in the activity of Fe/ZSM-5 towards N_2O decomposition. The optimum treatment temperature was determined as 750 °C. Fe–O with long bond lengths in the polynuclear amorphous FeOx species was the active species for N_2O decomposition. The amount of active FeO_x species was a key factor influencing the apparent activity of the Fe/ZSM-5 catalysts. When compared with the apparent activation energy E_a, the apparent pre-exponential factor A was more important in determining the reaction rate, where A depends on the total value of active entropy.

Acknowledgments

We thank Prof. Yu-ying Huang at Shanghai Synchrotron Radiation Facility (China) for making available synchrotron beam time for us to carry out XAFS measurement.

References

[1] Pérez-Ramírez J, Kapteijn F, Schöffel K, Moulijn J A. *Appl Catal B*, 2003, 44: 117
[2] Stott L, Poulsen C, Lund S, Thunell R. *Science*, 2002, 297: 222
[3] Pérez-Ramírez J, Kapteijn F, Mul G, Xu X D, Moulijn J A. *Catal Today*, 2002, 76: 55
[4] Pérez-Ramírez J, Kapteijn F, Mul G, Moulijn J A. *Appl Catal B*, 2002, 35: 227
[5] Pérez-Ramírez J, Kapteijn F, Mul G, Moulijn J A. *Chem Commun*, 2001: 693
[6] Sun K Q, Xia H A, Feng Z C, van Santen R, Hensen E, Li C. *J Catal*, 2008, 254: 383
[7] Sun K Q, Zhang H D, Xia H A, Lian Y X, Li Y, Feng Z C, Ying P L, Li C. *Chem Commun*, 2004: 2480
[8] Sazama P, Sathu N K, Tabor E, Wichterlova B, Sklenak S, Sobalik Z. *J Catal*, 2013, 299: 188
[9] Sazama P, Wichterlová B, Tábor E, Šťastny P, Sathu N K, Sobalik Z, Dědeček J, Sklenák S, Klein P, Vondrova A. *J Catal*, 2014, 312: 123
[10] Berlier G, Spoto G, Bordiga S, Ricchiardi G, Fisicaro P, Zecchina A, Rossetti I, Selli E, Forni L, Giamello E, Lamberti C. *J Catal*, 2002, 208: 64
[11] Ferretti A M, Oliva C, Forni L, Berlier G, Zecchina A, Lamberti C. *J Catal*, 2002, 208: 83
[12] Kiwi-Minsker L, Bulushev D A, Renken A. *J Catal*, 2003, 219: 273
[13] Dubkov K A, Ovanesyan N S, Shteinman A A, Starokon E V, Panov G I. *J Catal*, 2002, 207: 341
[14] Pérez-Ramírez J, Kapteijn F, Mul G, Moulijn J A. *Catal Commun*, 2002, 3: 19
[15] Sun K Q, Xia H A, Hensen E, van Santen R, Li C. *J Catal*, 2006, 238: 186
[16] Roy P K, Pirngruber G D. *J Catal*, 2004, 227: 164
[17] Zhu Q, van Teeffelen R M, van Santen R A, Hensen E J M. *J Catal*, 2004, 221: 575
[18] Zhu Q, Mojet B L, Janssen R A J, Hensen E J M, van Grondelle J, Magusin P C M M, van Santen R A. *Catal Lett*, 2002, 81: 205
[19] Hensen E J M, Zhu Q, Hendrix M M R M, Overweg A R, Kooyman P J, Sychev M V, van Santen R A. *J Catal*, 2004, 221: 560
[20] Perez-Ramirez J, Kapteijn F, Groen J C, Domenech A, Mul G, Moulijn J A. *J Catal*, 2003, 214: 33
[21] Perez-Ramirez J. *J Catal*, 2004, 227: 512
[22] Perez-Ramirez J, Mul G, Kapteijn F, Moulijn J A, Overweg A R, Domenech A, Ribera A, Arends I W C E. *J Catal*, 2002, 207: 113

Graphical Abstract

Chin. J. Catal., 2014, 35: 1972–1981 doi: 10.1016/S1872-2067(14)60184-4

Role of aggregated Fe oxo species in N_2O decomposition over Fe/ZSM-5

Bo Zhang, Fudong Liu, Hong He*, Li Xue
Research Center for Eco-Environmental Sciences, Chinese Academy of Sciences

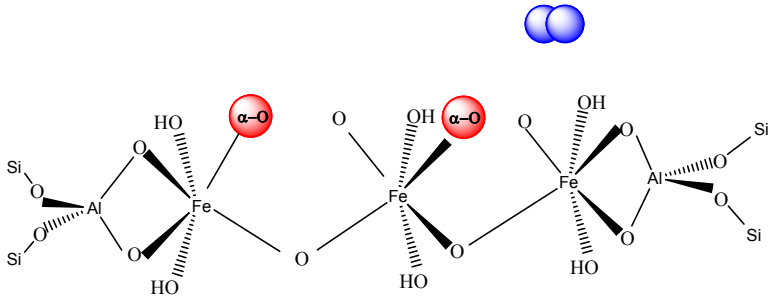

Fe–O species, with a long bond length, in polynuclear amorphous Fe oxo species are the real active species of Fe/ZSM-5 towards N_2O decomposition. Apparent pre-exponential factor is important to the reaction rate.

[23] Perez-Ramirez J, Groen J C, Brückner A, Kunar M S, Bentrup U, Debbagh M N, Villaescusa L A. *J Catal*, 2005, 232: 318
[24] Kaucký D, Sobalík Z, Schawarze M, Vondrová A, Wichterlová B. *J Catal*, 2006, 238: 293
[25] Joyner R, Stockenhuber M. *J Phys Chem B*, 1999, 103: 5963
[26] Pirngruber G D, Roy P K, Prins R. *J Catal*, 2007, 246, 147
[27] Pirngruber G D, Luechinger M, Roy P K, Cecchetto A, Smirniotis P. *J Catal*, 2004, 224: 429
[28] Koningsberger D C, Mojet B I, van Dorssen G E, Ramaker E E. *Top Catal*, 2000, 10: 143
[29] Sing K S W, Everett D H, Haul R A W, Moscou L, Pierotti R A, Rouquerol J, Siemieniewska T. *Pure Appl Chem*, 1985, 57: 603
[30] Perez-Ramirez J, Kumar M S, Brückner A. *J Catal*, 2004, 223: 13
[31] Battiston A A, Bitter J H, de Groot F M F, Overweg A R, Stephan O, van Bokhoven J A, Kooyman P J, van der Spek C, Vankó G, Koningsberger D C. *J Catal*, 2003, 213: 251
[32] The equitions quote from Wikipedia, the free encyclopedia. http://en.wikipedia.org/wiki/Arrhenius_equation
[33] McNaught A D, Wilkinson A. Compendium of Chemical Terminology, IUPAC. Blackwell Sci Inc, 1997